

# Long-term optical reliability and lifetime predictability of double clad fibers

Jaroslav Abramczyk, Harish Govindarajan, Wells Cunningham,  
Douglas Guertin and Kanishka Tankala

Nufern, 7 Airport Park Road, East Granby, CT 06026  
Phone: (860) 408 5000; FAX: (860) 408 5080

## ABSTRACT

With the use of fiber lasers pervading diverse applications and environmental conditions, the long-term reliability of low index (LI) polymer coated double-clad (DC) fibers used for this purpose is significant. Mechanical reliability standards for 125 $\mu$ m fibers are well established by Telcordia GR-20-CORE requirements and some work<sup>1</sup> has been published investigating optical reliability of DC fibers with specially engineered coatings with respect to accelerated temperature and humidity aging. While these are helpful in providing a figure of merit to the optical reliability of LI fluoroacrylate coatings, it becomes important to decouple the effects of temperature and humidity in order to understand the underlying degradation mechanisms of LI polymers in various storage and operating environments. This paper identifies the effects of temperature and humidity on the spectral attenuation of DC fibers and presents a reliability model capable of predicting lifetimes under prolonged exposure to typical temperature and humidity conditions experienced during storage and operation of fiber lasers.

## INTRODUCTION

Fiber lasers have become ubiquitous for a variety of material processing applications ranging from marking, engraving, micro-machining, cutting, and welding. The longevity of a fiber laser depends on the reliability of a variety of components in the system including the active and passive double clad fibers used to make the laser. While studying the reliability of the fiber, the reliability of the rare earth doped core as well as that of the cladding formed by silica glass encased in a low index fluoroacrylate polymer needs to be examined. Several researchers have studied both the photodarkening performance<sup>2,3,4</sup> and damage threshold of the glass at high laser powers. However, only limited amount of work has been conducted on studying the reliability of LI coated DC fibers<sup>1</sup>. Tankala et al.<sup>1</sup> have reported that the LI polymer serve both mechanical and optical functions, and the reliability of the fiber with respect to both functions needs to be addressed. They have demonstrated that well-engineered LI polymers can provide excellent tensile strength and stress corrosion parameter comparable to standard acrylate coatings used for telecommunication fibers and have also provided an accelerated test that can be used to engineer polymer coatings that have better resistance to temperature and humidity. Apart from this work the authors are not aware of any extensive analysis to understand the effects of temperature and humidity on the performance of double clad fibers. In addition, while there are mechanical reliability models available for polymer coated fibers that may be applicable to LI coated DC fibers, we are not aware of any reliability models that can predict the optical performance of LI coated double clad fibers.

Polymeric materials are known to degrade upon exposure to temperature and humidity. The low index polymer coating, encasing the cladding in a DC fiber, helps guide the pump light that can be absorbed by rare earth dopants in the core. The pump light used for ytterbium (Yb) or erbium (Er)/Yb co-doped fibers are typically 915 nm, 940 nm or 976 nm while that used for thulium (Tm) doped fibers is around 793 nm. In order to understand the impact of temperature and humidity on the ability of the LI polymer to reliably guide the pump light, changes in spectral attenuation in a wavelength band encompassing these specific wavelengths, and their contribution to loss at the specific pump

wavelengths, needs to be studied. Furthermore, development of a model that predicts the attenuation increase at specific wavelengths requires extensive experimental data that provides insight into the individual effects of temperature and humidity. A prerequisite to conducting a carefully thought out experimental plan and collecting such an extensive data set to develop a predictive model is to have a well-engineered and consistent low index fluoroacrylate material which will give repeatable data.

This paper presents a well-engineered low index polymer that has significantly improved and consistent performance to both dry (< 1% relative humidity) and damp heat. With the aid of a well thought out experimental matrix of temperature and humidity conditions the authors are able to present the key factors contributing to the attenuation changes at typical pump wavelengths. Further, the paper analyzes the rate of increase of attenuation, with diffusion and Arrhenius analysis, and presents a rigorous model for predicting the experimentally observed attenuation changes. Finally, the authors use examples of storage and operating conditions to elucidate the significance of such conditions on laser system lifetime.

### SELECTION OF LOW INDEX POLYMER AND DESIGN OF EXPERIMENTS

A coreless passive 125 micron clad fiber, MM-125-FA, was selected for evaluating a suitable low index polymer and determining the key factors influencing optical attenuation upon exposure to temperature and humidity. The 125 micron optical grade glass is coated with a low index fluoroacrylate and further encased in a telecom grade standard acrylate coating for providing mechanical protection to the low index polymer. A 125 micron fiber was chosen as it represents a worst case scenario for changes in optical attenuation. Pump light in larger diameter fibers experiences less interaction with the polymer coating per unit length and the changes in attenuation are inversely proportional to the diameter of the fiber. Two low index fluoroacrylate materials – a commercially available coating (CAC) and a low index polymer specially engineered for improved performance (NuCOAT<sub>FA</sub>) were evaluated for optical performance when exposed to damp heat (60 °C and 85% RH) and dry heat (85 °C and 1 % RH).

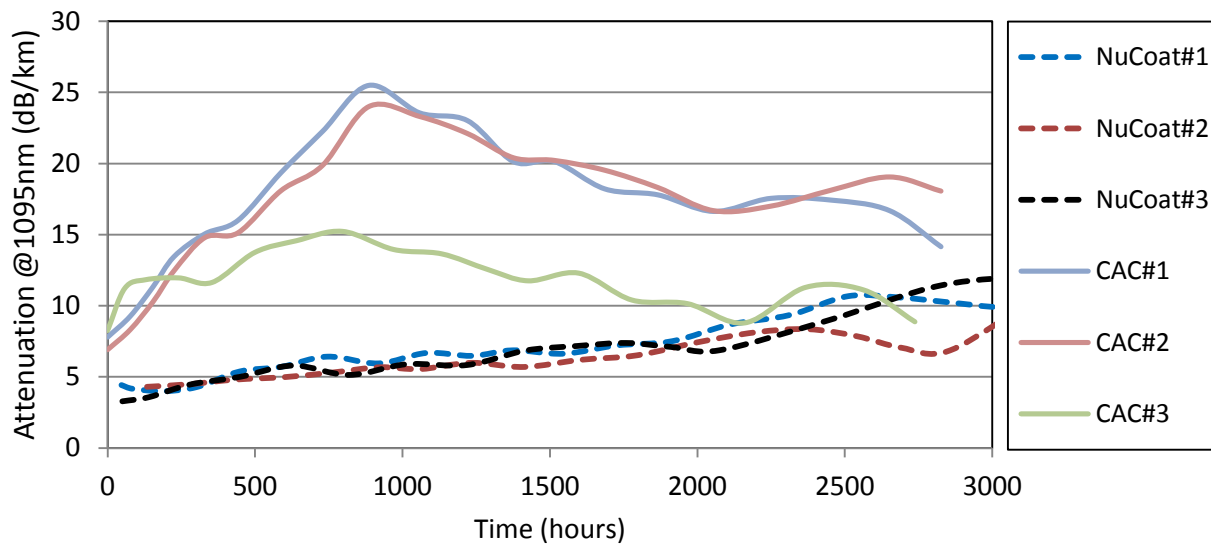


Figure 1: Comparative attenuation performance of NuCOAT<sub>FA</sub> vs. CAC in a damp-heat environment.

The attenuation change at 1095 nm as a function of time of exposure to 60 °C and 85% RH is presented in Figure 1. Three lots each of a CAC and NuCOAT<sub>FA</sub> were tested for determining statistically significant differences in performance and evaluating the consistency in performance. As can be observed, NuCOAT<sub>FA</sub> performed significantly

better, exhibiting < 10dB/km attenuation change even after 3000 hours while the CAC shows attenuations as high as 25 dB/km in less than 1000 hours. In addition, the performance of multiple lots of NuCOAT<sub>FA</sub> is very repeatable. The authors note that fibers with CAC appear to recover in performance upon continued exposure. A better coating system is one which maintains low attenuation for the longest time.

Similarly, the performance of the two coatings in dry heat environment of 85 °C and 1% RH was evaluated and the data is presented in Figure 2. Once again it is clear that NuCOAT<sub>FA</sub> exhibits virtually no increase in attenuation at 1095 nm while fibers with CAC can deteriorate to >30 dB/km in 1500 hours. Once again the authors note that the NuCOAT<sub>FA</sub> system exhibits remarkable consistency in performance. The experimental observations indicate that polymer coatings can be engineered to provide improved and consistent optical reliability. In addition, owing to its repeatable performance, NuCOAT<sub>FA</sub> is a good candidate for undertaking a systematic experimental study to understand the effects of temperature and humidity on optical attenuation of DC fibers.

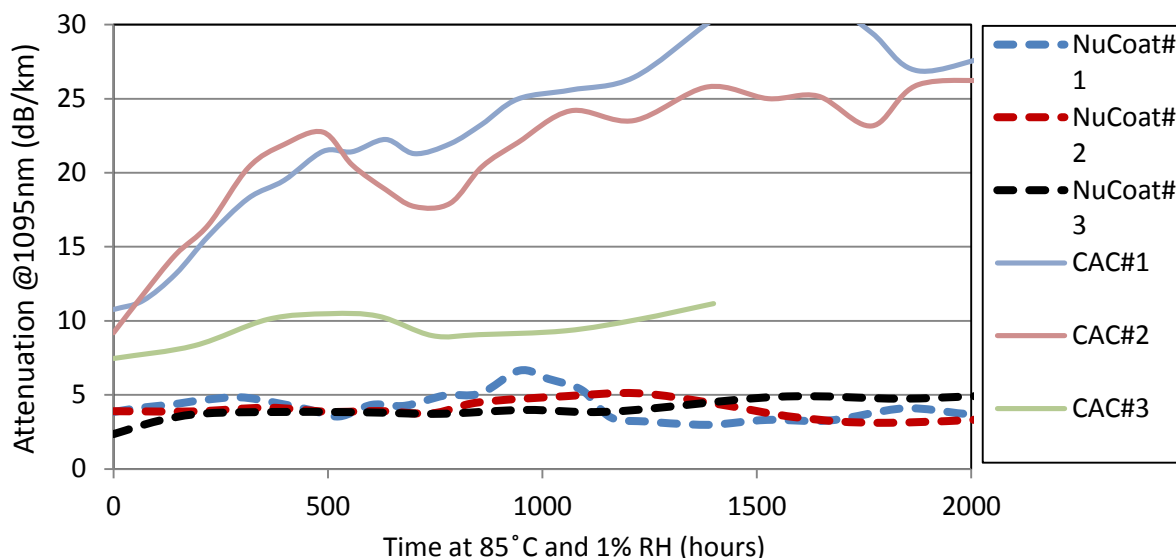


Figure 2: Comparative attenuation performance of three lots each of NuCOAT<sub>FA</sub> vs. CAC in a dry-heat environment.

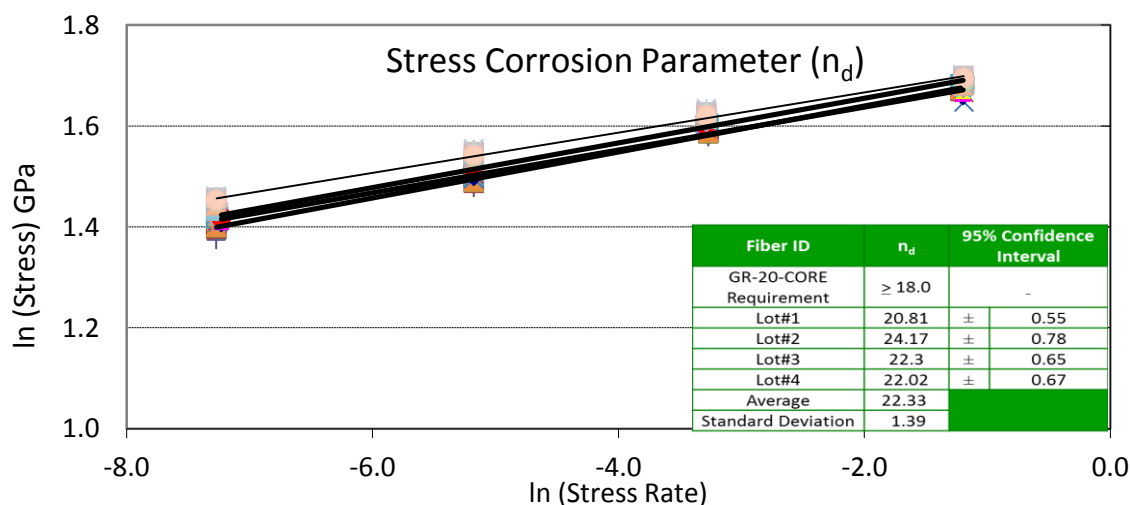


Figure 3: Stress Corrosion Parameter for MM-125-FA with NuCOAT<sub>FA</sub>.

Mechanical reliability of acrylate coated fibers has been extensively studied and well documented<sup>5,6,7</sup>. Fibers with NuCOAT<sub>FA</sub> exhibit exceptional stress corrosion parameter,  $n_d$ , of > 22 (Figure 3) and tensile strengths of > 700 kpsi without low strength breaks (Figure 4). It can therefore be considered a high strength fiber and established methods<sup>4</sup> of analyzing mechanical reliability can be used to predict long term mechanical performance of LI coated DC fibers.

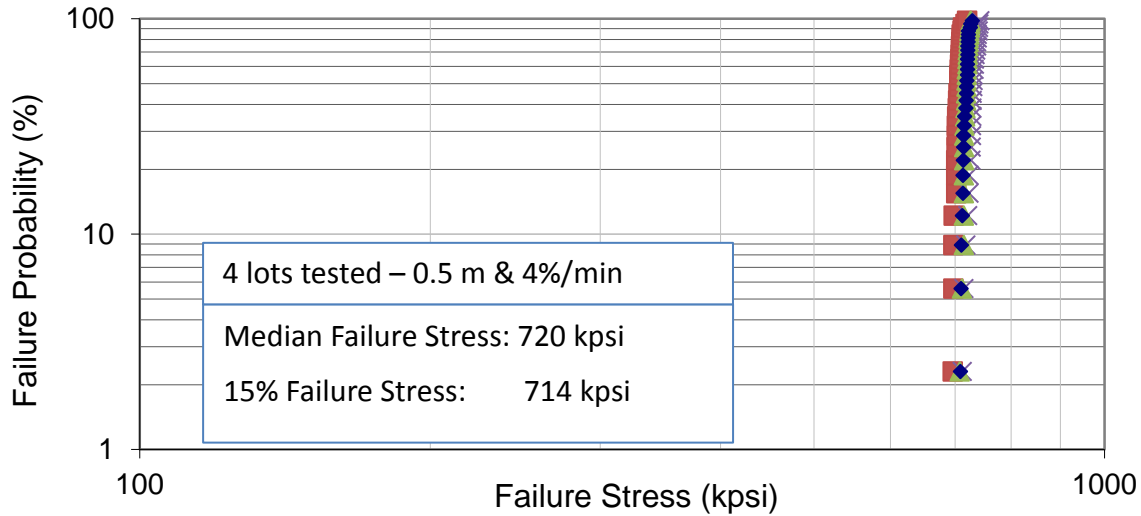


Figure 4: Dynamic Tensile Strength, MM-125-FA with NuCOAT<sub>FA</sub>

An MM-125-FA fiber drawn with NuCOAT<sub>FA</sub> was used to monitor the changes in spectral attenuation in the 700 to 1100 nm region under various temperature and humidity conditions. The experimental conditions chosen to investigate temperature and humidity effects are presented in Table 1. A dry heat environment with < 1% RH was chosen to determine the effect of temperature on the spectral attenuation. The humidity was varied from <1 % RH to 95% RH at a fixed temperature of 85 °C to understand the effect of humidity. Furthermore, to study the impact of temperature related effects at elevated humidity levels, the temperature was varied from 60 °C to 95 °C at a fixed relative humidity of 85%.

Table 1: Experimental conditions chosen (marked by X) to understand the effects of temperature and humidity on spectral attenuation and develop a predictive model for fiber life time.

	60 °C	85 °C	95 °C	125 °C	150 °C	175 °C
< 1% RH		<b>X</b>		<b>X</b>	<b>X</b>	<b>X</b>
40 % RH		<b>X</b>				
60 % RH		<b>X</b>				
85 % RH	<b>X</b>	<b>X</b>	<b>X</b>			
95 % RH		<b>X</b>				

## RESULTS AND DISCUSSION

Spectral attenuation changes upon exposure to 85 °C and 85% RH are presented in Figure 5. We observed that the attenuation changes due to temperature and humidity exposure can be represented as a sum of three distinct processes that can each be easily isolated and evaluated. We define attenuation increase due to the three contributors as follows:

- $\Delta\alpha_T$ : Wavelength dependent loss at low wavelength related purely to the effect of temperature exposure on the fiber. We will also refer to it as attenuation due to “Dry Heat”.
- $\Delta\alpha_{OH}$ : Increase in attenuation due to diffusion of moisture into silica cladding and formation of Si-OH. While diffusion rates are affected by temperature the effect is due to humidity.
- $\Delta\alpha_S$ : Wavelength independent loss related to scattering at the glass-coating interface. It will be shown that this effect is purely due to humidity.

The total change in attenuation at any pump wavelength ( $\Delta\alpha_\lambda$ ), as a function of time, temperature and humidity, can be represented as the sum of these three contributions:

$$\Delta\alpha_\lambda = \Delta\alpha_T + \Delta\alpha_{OH} + \Delta\alpha_S \quad (1)$$

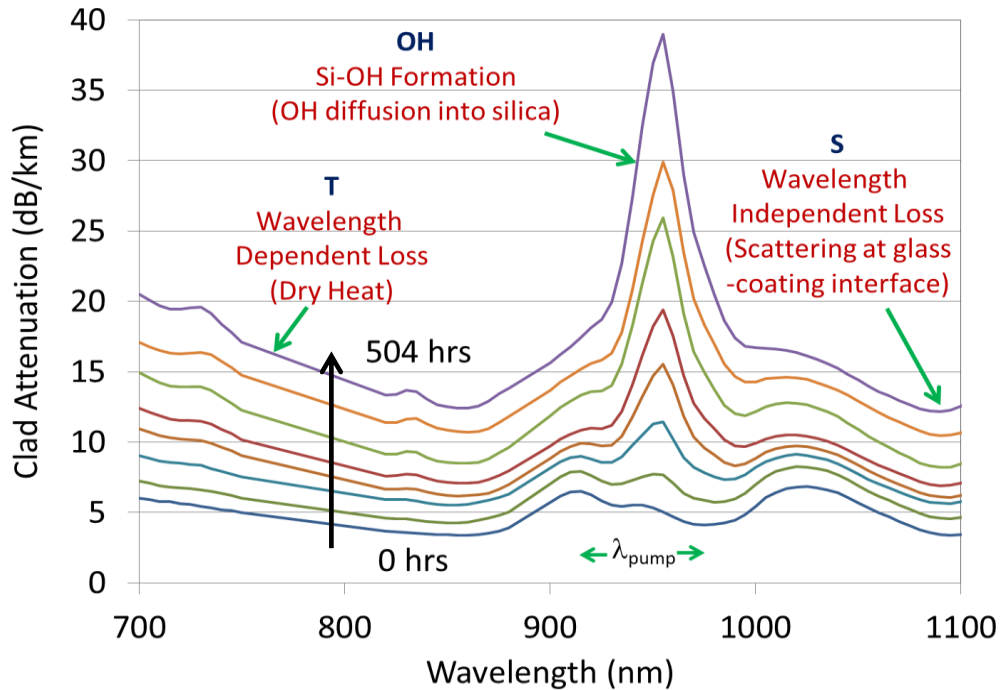


Figure 5: Spectral Attenuation increase over time at 85 °C and 85% R.H.

### Effect of temperature on attenuation

In order to determine the effect of temperature we examined the changes in attenuation at different temperatures with time at very low humidity levels of <1 % RH. Figure 6 shows the spectral attenuation changes with time at 150 °C. The solid lines are the exponential fit to the measured data points. It is observed that the experimental data can be represented very well by an exponential function. The attenuation at 955 nm and nearby wavelengths deviates a little due to the contribution due to Si-OH formation even at these low humidity levels. We observe that the exponential fit to the short wavelength attenuation is a better estimate of the temperature contribution to attenuation rather than the direct

experimental measurement which has some contribution from the attenuation due to Si-OH formation. By analyzing the attenuation changes with time for 85 °C, 125 °C, 150 °C and 175 °C we are able to find the following relationship for the attenuation at a desired pump wavelength:

$$\Delta\alpha_T(\lambda) = \Delta\alpha_{T,700\text{nm}} * \exp \{ - 0.0103 (\lambda-700) \} \quad (2)$$

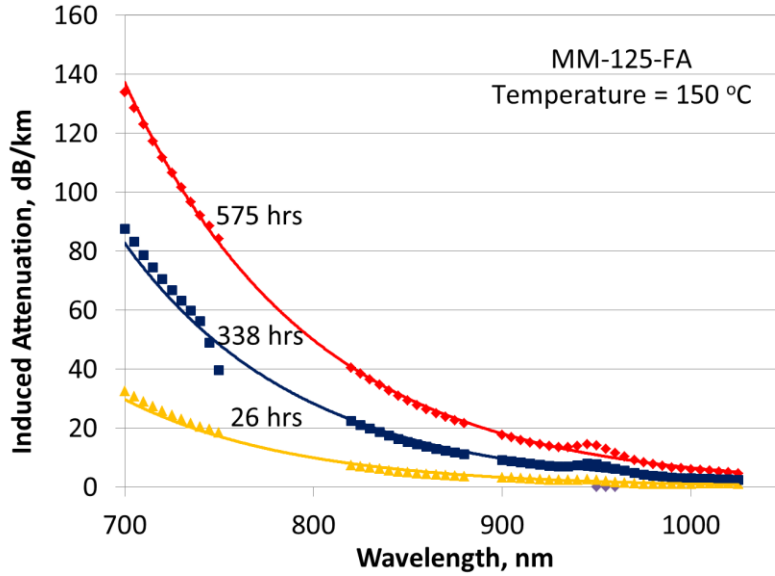


Figure 6: Attenuation performance of NuCOAT<sub>FA</sub> at 150°C dry-heat

This exponential relationship in equation (2) was used to determine the induced attenuation at pump wavelengths for any given time and temperature based on the experimentally measured attenuation change at 700 nm. Figure 7 presents the changes in 915 nm attenuation as a function of time for various temperatures. It is apparent that the increase in attenuation is a strong function of temperature. A closer examination of the induced attenuation shows different regimes of attenuation change with time. The different regimes can be clearly seen especially in the 125 °C data. The attenuation increases initially at a fast rate,  $k_{TF}$ , and after certain time, defined as fast period,  $\tau_{FL}$ , the attenuation reaches a certain value which we define as fast limit,  $\Delta\alpha_{FL}$ , after which the attenuation increases at a slow rate,  $k_{TS}$ .

If temperature dependencies of the fast rate, fast limit and slow rate can be determined, the temperature contribution to attenuation change at any time and temperature can be predicted. To determine the temperature dependencies of these parameters Arrhenius plots of the logarithm of rate vs  $1/T$  are plotted. A linear fit to the data indicates that a single process is at play and is characterized by activation energy,  $E_a$ . The slope of the Arrhenius plots provides  $E_a/k$ , where  $k$  is the Boltzmann's constant, and the intercept provides the pre-exponential constant. Figure 8 shows Arrhenius plots for the fast and slow rates, respectively. The excellent linear regression of both these parameters shows that there is a unique process involved for each of these rates and they follow typical Arrhenius relationships as shown in equations (3) and (4). Similarly, an Arrhenius relationship was found for the fast limit and is presented in equation (5). The fast time limit can be estimated from the fast rate and the fast limit values as shown in equation (6). The induced attenuation at 915 nm as a function of temperature for a desired time,  $t$ , can be predicted based on equations (7) and (8) for time periods less than or greater than the fast time limit, respectively.

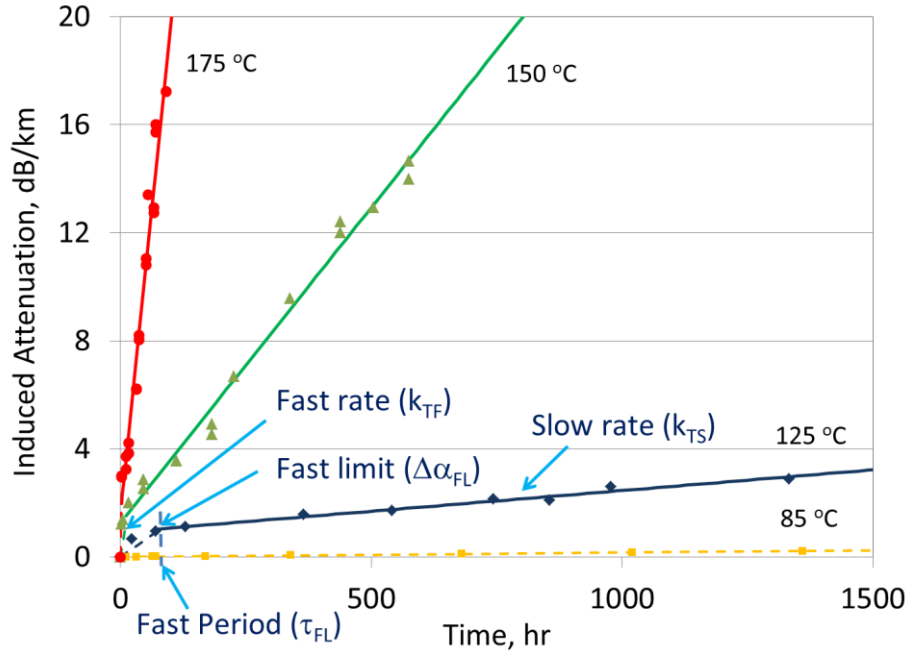


Figure 7: The change in attenuation, at 915 nm, with time for a 125 μm fiber coated with NuCOAT<sub>FA</sub> under dry-heat-exposure.

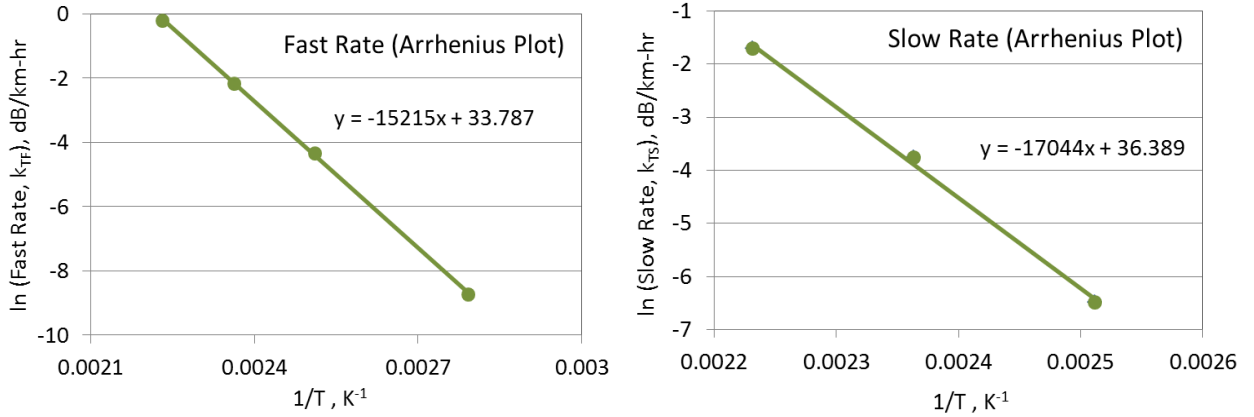


Figure 8: Arrhenius plots for the fast rate and the slow rate.

$$K_{TF} = 4.72 * 10^{14} \exp \left\{ \frac{-15215}{T} \right\} \quad (3)$$

$$K_{TS} = 6.36 * 10^{15} \exp \left\{ \frac{-17044}{T} \right\} \quad (4)$$

$$\Delta\alpha_{FL} = 144 \exp \left\{ \frac{-2009}{T} \right\} \quad (5)$$

$$\tau_{FL} = \Delta\alpha_{FL} / k_{TF} \quad (6)$$

$$\Delta\alpha_{T, 915} = k_{TF} * t \quad \text{for } t < \tau_{FL} \quad (7)$$

$$\Delta\alpha_{T, 915} = \Delta\alpha_{FL} + k_{TS} * (t - \tau_{FL}) \quad \text{for } t > \tau_{FL} \quad (8)$$

The temperature dependent induced attenuation at other wavelengths can be expressed as a function of the attenuation change at 915 nm using the exponential relationship similar to Equation (2) as shown in Equation (9). The  $\Delta\alpha_{T,915}$  values in Equations (7) and (8) can be used in Equation 9 to get temperature induced attenuation change at other pump wavelengths.

$$\Delta\alpha_T(\lambda) = \Delta\alpha_{T,915} * \exp \{ -0.0103 (\lambda-915) \} \quad (9)$$

### Effect of moisture diffusion into silica (Si-OH formation) on attenuation

The moisture present in the ambient can diffuse through the polymer coating and into the glass<sup>8</sup> with time (Figure 9). This moisture can react with the silica to form Si-OH which has a characteristic absorption peak around 955 nm which effects the attenuation of nearby pump wavelengths of 915, 940 and 976 nm. The moisture in the ambient atmosphere can diffuse rapidly through the polymer and reach the glass/polymer interface. It is therefore safe to assume that there is minimal gradient in concentration of water vapor through the polymer and the concentration at the glass surface can be approximated to be proportional to the ambient water vapor density. The ambient vapor density can be calculated from well-known saturation vapor density defined by ambient temperature,  $T_A$ , and the relative humidity, %RH, as shown in equation (10).

$$\rho_{H_2O} [g/m^3] = \%RH * [6.335 + 0.6718 * T_A - 2.0887E-2 * T_A^2 + 7.3095E-4 * T_A^3] \quad (10)$$

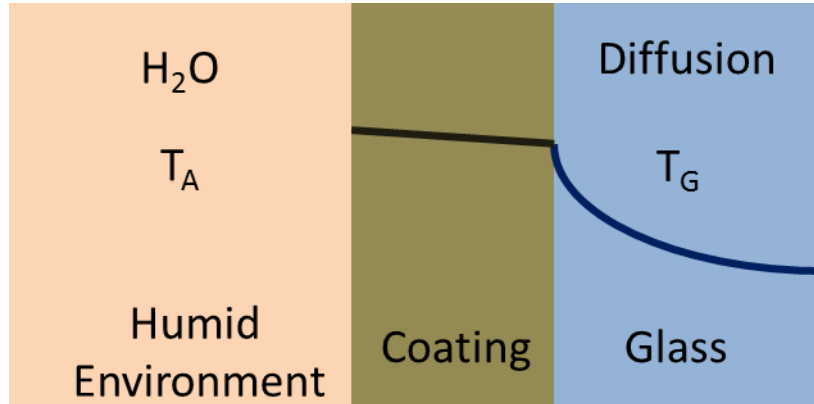


Figure 9: Schematic of moisture diffusion through the polymer coating and glass cladding.

We have observed that the absorption peak at 955 nm can be represented very well by a Lorentzian function with a half width at half max value of 15 nm. Hence, the attenuation at wavelengths around 955 nm can be expressed as a function of measured attenuation at 955 nm by the Lorentzian function in Equation (11).

$$\Delta\alpha_{OH}(\lambda) = \Delta\alpha_{OH,955} * (15)^2 / \{ (\lambda - 955)^2 + (15)^2 \} \quad (11)$$

The attenuation increase due to Si-OH formation should be proportional to the surface concentration of water and the diffusion and reaction of moisture to form Si-OH. Figure 10 shows the experimentally measured rate (at 915 nm) versus vapor density for various relative humidity values at a constant temperature of 85°C. Since the rate shows a linear dependence with vapor density, the temperature dependence of this rate can be obtained from an Arrhenius plot of the rate normalized to vapor density (Figure 11).

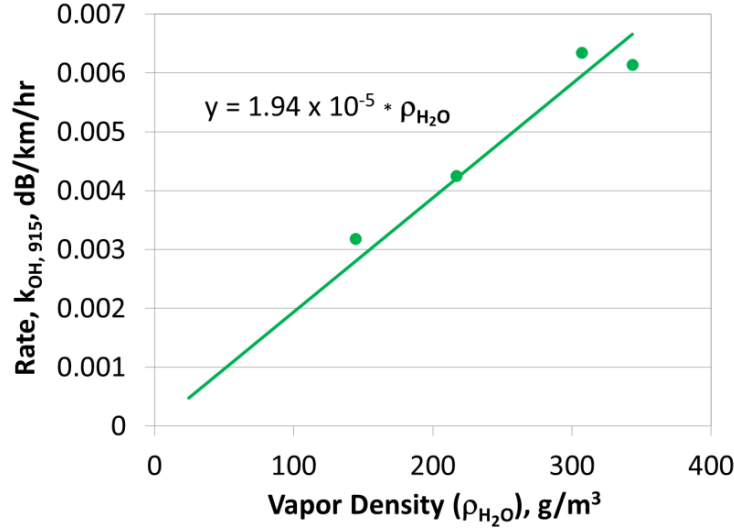


Figure 10: The dependence of attenuation on vapor density for fixed temperature of 85°C.

Figure 11 presents the normalized rate of increase in attenuation as a function of  $1/T$  for various temperature and relative humidity combinations. A linear fit to the data indicates a single rate determining process with unique activation energy. Since the experiments were conducted in a temperature humidity chamber the ambient temperature and the glass temperature are the same. In typical storage conditions the ambient and glass temperatures can be approximated to be the same. During operation however, the quantum defect heating of the fiber may make the glass temperature different than the ambient temperature. We therefore define a glass temperature,  $T_G$ , which will govern the diffusion of moisture into the silica cladding, as distinct from the ambient temperature,  $T_A$ . For the analysis of the experimental data and establishing the temperature dependence of rate, we use the chamber temperature for both the ambient and glass temperature. For the users of the model, ambient temperature should be used for determining vapor density, as shown in equation (10) while fiber temperature should be used for diffusion and reaction of moisture to form Si-OH as shown in equation (12). Based on the relationships observed in Figure 10 and 11 the induced attenuation due to Si-OH formation can be expressed as follows:

$$\Delta\alpha_{OH,915} = 663 * \rho_{H2O} * \exp\left\{\frac{-6198}{T_G}\right\} * t \quad (12)$$

The attenuation increase due to Si-OH formation for any wavelengths around 955 nm can be derived by re-writing Equation (11)

$$\Delta\alpha_{OH}(\lambda) = 8.12 * \Delta\alpha_{OH,915} * (15)^2 / \{ (\lambda - 955)^2 + (15)^2 \} \quad (13)$$

### Effect of moisture on induced attenuation due to scattering at glass/coating interface

The experimentally measured rate of increase in scattering losses was plotted as a function of vapor density for various combinations of temperature and humidity conditions in Figure 12. While the authors do not understand the mechanism for the formation of scattering sites at this time, we see a remarkable quadratic dependence of rate to vapor density. The data indicates that two water molecules are critical to formation of a scattering site.

The contribution to pump attenuation due to this scattering induced loss,  $\Delta\alpha_s$ , can be estimated based on the experimentally observed dependence of rate as shown in equation (14):

$$\Delta\alpha_s = 1.9E-07 * \rho_{H2O}^2 * t \quad (14)$$

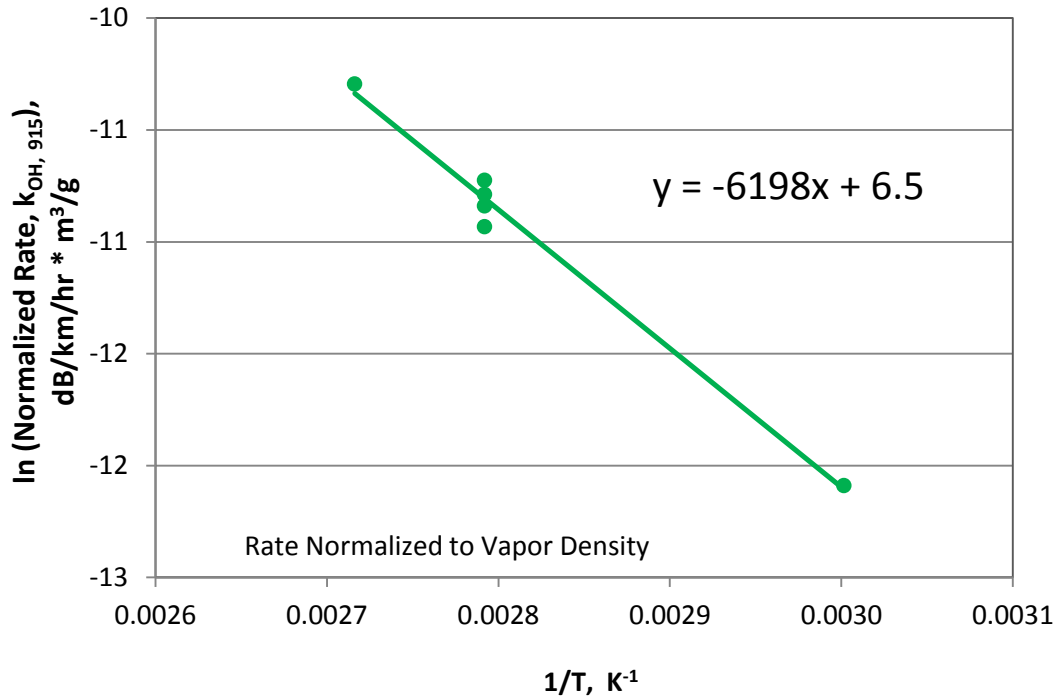


Figure 11: Arrhenius plot of normalized (to vapor density) rate of increase in attenuation at 915 nm.

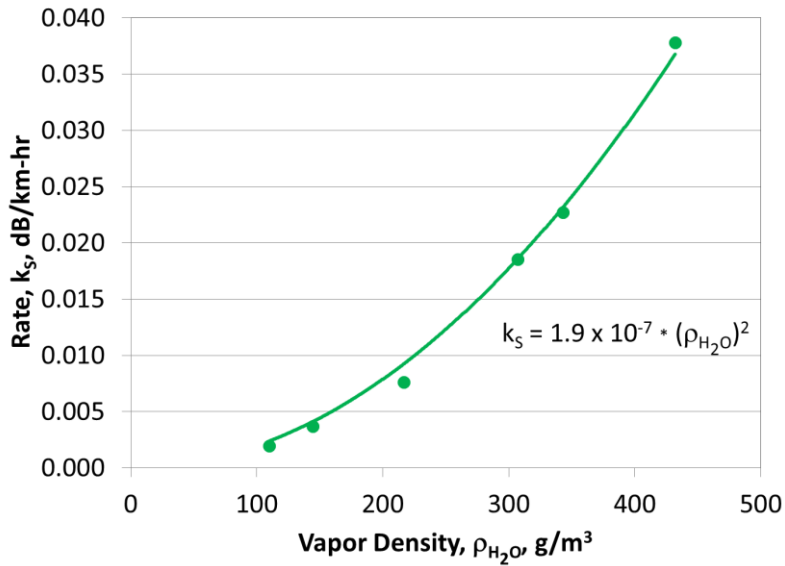


Figure 12: Rate of increase in wavelength independent attenuation versus vapor density.

### Experimental verification of the model

As discussed earlier, the total attenuation, as expressed in Equation (1), after any period of time and exposure condition can be predicted within the spectral band of 700 nm to 1100 nm by using the attenuation of the unexposed fiber and the cumulative effects of the three contributors to attenuation change. The accuracy of the model was verified by comparing the predicted value to the experimental data after the longest exposure time we have. Figure 13 shows the

attenuation spectrum of the unexposed fiber, the calculated contribution of temperature ( $\Delta\alpha_T$ ), Si-OH formation ( $\Delta\alpha_{OH}$ ), and scattering loss ( $\Delta\alpha_S$ ) for a fiber exposed to 60 °C and 85% RH for 2744 hours. The predicted attenuation spectrum generated from the sum of the loss of unexposed fiber and the three contributions is compared with the experimentally measured spectrum. As can be observed from Figure 13, the predicted data is in excellent agreement with experimental data indicating that all key degradation mechanisms have been adequately accounted and rigorously incorporated into the model.

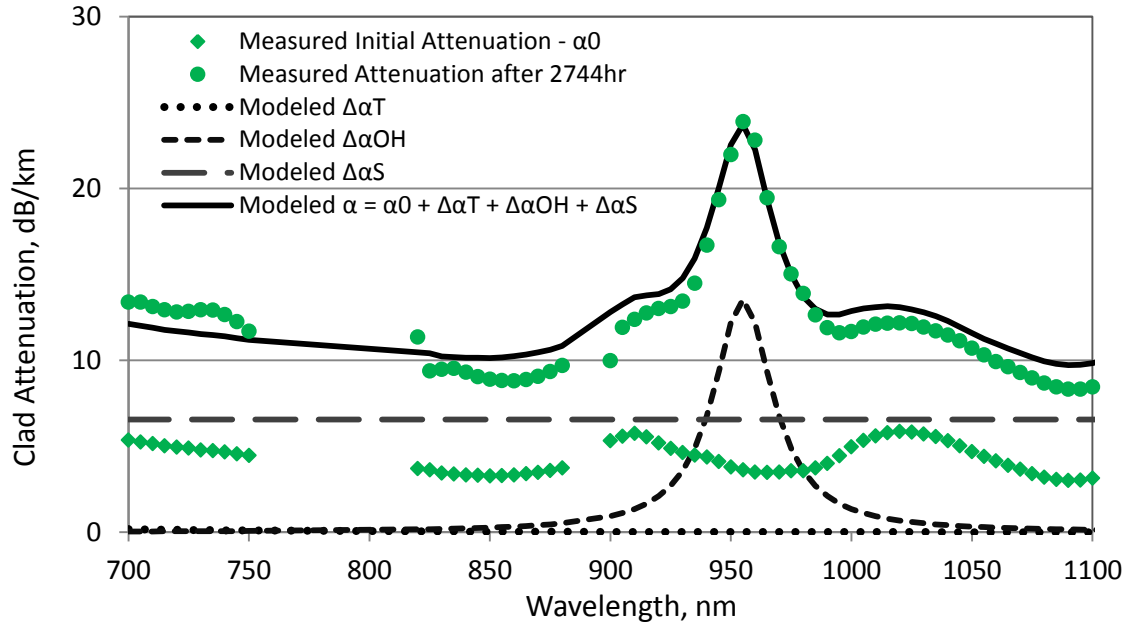


Figure 13: Comparison of attenuation spectrum predicted by the model with the experimentally measured spectrum. Model predictions and experimental data is for 2744 hours at 60 °C and 85 %RH.

### Lifetime predictions and significance of the model

Laser manufacturers typically design their systems with some performance margin. It is not uncommon for the system to have 20% higher power margin as the product is shipped to customers. The laser system is expected to have a lifetime and this margin provides for degradation of individual components in the system including the DC fiber. Laser manufacturers will have to allocate the margin for degradation of each component. We conduct a simplistic analysis where we estimate the lifetime of the laser system if the entire margin is allocated to degradation of the active fiber. We consider an example of a fiber with 0.4 dB/m pump absorption at 915 nm. Thirty three meters (33 m) of such fiber would have to be used to absorb 95% of the pump light. If the system has a 20% margin in power, the fiber can experience 1 dB total induced loss at 915 nm, for the 33 m device length, before the laser will fail to meet the power specification for the system. This 1 dB induced loss, for a 33 m device length, is equal to a 30 dB/km increase in loss. Table 2 presents system life time in years for various conditions that will result in 30 dB/km induced loss.

For a laser system that is operating in an ambient conditions of 25 °C and 40% RH and the active fiber is at 40 °C (due to quantum defect heating and despite measures to cool the fiber), data in Table 2 indicates that if the entire laser system margin of 20% is allocated to the active fiber the system lifetime would be over 118 years. In reality of course, allowances have to be made for degradation of other components and only a fraction of the laser system margin will be available for the active DC fiber.

Table 2: Time to failure for 33m device pumped at 915nm, pump absorption of the fiber 0.4dB/m. Failure criterion 20%.

	$T_A$ ( °C )	$T_G$ ( °C )	RH (%)	Time (years) Continuous Exposure
Typical Conditions	25	40	40	118
Elevated Condition A	40	40	85	9.4
Elevated Condition B	40	55	85	7.3
Temperature Only	40	100	1	30

Some laser manufacturers define the maximum ambient temperature and humidity that the laser should be operated as 40 °C and 85% RH. If we assume that system runs at this extreme condition continuously, and the active fiber can be maintained at 40 °C, the system lifetime would be over 9 years. If the active fiber cannot be maintained at 40 °C but has a 15 °C delta over the ambient, the system life time would reduce to over 7 years. Since continuous operation at such ambient conditions of 40 °C and 85 % RH is unlikely, there should be adequate margin available for degradation of other components. Finally we point out that the critical factor effecting life time is the humidity rather than temperature. Table 2 shows that if the fiber is operated at a temperature of 100 °C and the laser manufactures successfully limit the exposure of fiber to humidity of < 1% RH the laser system would last for 30 years. The data in Table 2 indicates that laser manufacturers can maximize system lifetime by providing adequate airflow for cooling, heat sinking the active fiber well to extract heat to keep its temperature low, and if possible minimizing the exposure of the DC fiber to humidity.

## CONCLUSION

A proprietary low index polymer coating, NuCOAT<sub>FA</sub>, with improved resistance to dry and damp heat performance compared to a commercially available coating has been developed. The repeatable and consistent performance of this coating has allowed the authors to explore the effects of temperature and humidity on the spectral attenuation and in particular the induced attenuation at typical pump wavelengths used for fiber lasers. For the first time, the key factors contributing to spectral attenuation changes upon exposure to temperature and humidity have been identified and a rigorous model that can predict the performance of the fiber has been developed. The predictive model can be used by laser manufacturers to determine the impact of temperature and humidity conditions experienced during storage and operation on the system lifetime as well as engineer the system for longevity.

## REFERENCES

1. Tankala, K., Guertin, D., Abramczyk, J and Jacobson, N., “Reliability of low-index polymer coated double-clad fibers used in fiber lasers and amplifiers”, *Optical Engineering*, 50(11), 111607 (2011)
2. Koponen, J., Soderlund, M., Hoffman, H. J., Kliner, D. A. V., Koplrow, J. P. and Hotoleanu, M., “ Photodarkening rate in Yb-doped silica fibers,” *Applied Optics*, 47(9), 1247 (2008).

3. Jetschke, S., Unger, S., Schwuchow, A., Leich, M. and Kirchhof, J., "Efficient Yb laser fibers with low photodarkening by optimization of the core composition," *Optics Express*, 16(20), 15540 (2008).
4. Rydberg, S. and Engholm, M., "Experimental evidence of the formation of divalent Ytterbium in the photodarkening process of Yb-doped fiber lasers," *Optics Express*, 21(6), 6681 (2013).
5. Mrotek, J. L., Matthewson, M. J., and Kurkjian, C. R., "Diffusion of Moisture through Fatigue and Aging-Resistant Polymer Coatings on Light guide Fibers", *J. Lightwave Technol* 21, 1775 (2003).
6. Armstrong, J. L., Matthewson, M. J., and Kurkjian, C. R., "Humidity Dependence of the Fatigue of High-Strength Fused Silica Optical Fibers", *Journal of the American Ceramic Society*, 83(12), (2000).
7. Griffioen, W., Breuls, A., Cocito, G., Dodd, S., Ferri, G., Haslov, P., Oksanen, L., Stockton, D. J., Svensson, T. K., "COST 218 evaluation of optical fiber lifetime models". *SPIE* 1791, (1993).
8. Doremus, R. H., "Diffusion of water in silica glass", *Journal of Materials Research*, 10(9), (1995).